

This work was written as part of one of the author's official duties as an Employee of the United States Government and is therefore a work of the United States Government. In accordance with 17 U.S.C. 105, no copyright protection is available for such works under U.S. Law.

Public Domain Mark 1.0

<https://creativecommons.org/publicdomain/mark/1.0/>

Access to this work was provided by the University of Maryland, Baltimore County (UMBC) ScholarWorks@UMBC digital repository on the Maryland Shared Open Access (MD-SOAR) platform.

Please provide feedback

Please support the ScholarWorks@UMBC repository by emailing scholarworks-group@umbc.edu and telling us what having access to this work means to you and why it's important to you. Thank you.

Shinnery Oak Bidirectional Reflectance Properties and Canopy Model Inversion

Donald W. Deering, Thomas F. Eck, and Toby Grier

Abstract— The fact that most plant communities exhibit anisotropic reflectance properties is currently well recognized. However, the nature of such reflectances and the diurnal and seasonal variations of bidirectional reflectance for natural plant communities are not well understood. Plant canopy models are being developed which will enable us to utilize this anisotropic property of vegetation to extract important plant information from remote sensing measurements. This paper presents field measurements and the results of a three-dimensional canopy model inversion for sand shinnery oak. Spectral bidirectional radiance measurements in three spectral channels, 0.65–0.67 μm , 0.81–0.84 μm , and 1.62–1.69 μm , encompassing both the complete land surface and sky hemispheres were acquired for a sand shinnery oak plant community in West Texas. The changes in canopy reflectance that occur with variations in solar zenith angle and view direction and for two seasons of the year were evaluated. A Three-dimensional Radiation Interaction Model (TRIM) was then inverted to estimate oak leaf area index (LAI) and canopy density, expressed as percentage cover, from the bidirectional reflectance data.

I. INTRODUCTION

In this study we focus on a single vegetation community type with the objective of gaining an increased understanding of the dynamics of the bidirectional reflectance at the canopy level. We also utilize measured bidirectional reflectance data in a canopy reflectance model in order to invert the model to obtain estimates of biophysical canopy parameters. Measurements of the visible and near-infrared reflectance were made with the PARABOLA instrument [1] over a wide range of solar zenith angles and in two distinct stages of the vegetation growing season. The vegetation community which we analyze here, a stand of sand shinnery oak is a semiarid plant community growing in West Texas. The study of the reflectance dynamics of semi arid ecosystems is important due to the increased utilization of satellite data to monitor these areas for changes in vegetation distribution [2] and to infer biophysical parameters of climatic significance [3].

Changes in the bidirectional reflectance as a function of solar zenith angle are often significant [4]–[8] and increased understanding of the mechanisms involved in the dynamics of

these changes is required in order to more accurately utilize remotely sensed measurements from satellite over vegetated surfaces. The variation in solar zenith angle occurs as a function of time of day of satellite overpass, latitude, and day of the year. Therefore, the effects of solar zenith angle induced changes in reflectance and associated vegetation indices are important in comparison of measurements between different satellites with different overpass times, comparison of measurements made on the continental scale and thus having a variation in solar zenith angle with latitude, and in the seasonal variation of a fixed location with the same satellite overpass time. In this paper we apply a simple geometrical model to study the relationship between plant canopy absorption with resultant shadowing and the visible canopy reflectance, as a function of solar zenith angle. Since the field measurements were acquired considerably in advance of the development of the models applied in this study, it must be noted that a rigorous sampling of all of the biophysical parameters needed to comprehensively examine a plant canopy model and its inversion accuracy was not accomplished. Nevertheless, the data were considered to be more than adequate to provide a valuable first test of the ability of the models to represent a naturally occurring semiarid vegetation type.

II. INSTRUMENTATION AND MEASUREMENT TECHNIQUES

A. Field Instruments

Field measurements of bidirectional canopy reflectance were acquired for this study using the Portable Apparatus for Rapid Acquisition of Bidirectional Observations of the Land and Atmosphere, called the PARABOLA. This instrument has been described in detail by Deering and Leone [1]. In summary, the PARABOLA is a two-axis scanning head three-channel (visible, near-infrared and mid-infrared; 650–670 nm, 810–840 nm and 1620–1690 nm, respectively), motor-driven radiometer that enables the acquisition of radiance data for almost the complete (4π) sky- and ground-looking hemispheres in 15° instantaneous field-of-view sectors in only 11 s. For this study the PARABOLA instrument was mounted on a lightweight, collapsible boom apparatus, which was anchored to the bed of a pickup truck.

Three complete PARABOLA replicate samples were averaged for each viewing angle measurement in the current study to minimize the within-field inhomogeneity effects. Three subsamples were adequate in this study, as the canopy sampled was chosen to be homogeneous and the measurement pixel instantaneous fields of view were large (ranging

Manuscript received September 26, 1991; revised November 7, 1991. This work was supported in part through the Remote Sensing Science Program of NASA Headquarters within the Earth Sciences and Applications Division and a NASA Graduate Researcher Fellowship sponsored by NASA's Goddard Space Flight Center.

D. W. Deering is with the Biospheric Sciences Branch/923, NASA Goddard Space Flight Center, Greenbelt, MD 20771.

T. F. Eck is with the Hughes STX Corporation, Lanham, MD 20706.

T. Grier is with the Department of Systems Science, State University of New York, Binghamton, NY 13901.

IEEE Log Number 9105848.

0196-2892/92\$03.00 © 1992 IEEE

from approximately 2 m² at nadir to 57 m² at a 45° off-nadir angle) relative to the canopy spatial structure. The average of the three values was taken as the canopy radiance for a particular view direction. Directional reflectances were computed as hemispherical-directional reflectance factors using the PARABOLA directional radiance measurements from the ground-looking hemisphere divided by the PARABOLA-derived incident irradiance as described in Section II.B.

A camera mounted near the PARABOLA scanning head provided for photographic documentation of the ground hemisphere target. A wide-angle (23 mm) lens with an "ultra-wider" adaptor was used to provide fisheye-like 35-mm photographs, which were used to determine the cover classes and percentages as described in Sections III and IV.A.

A Sun photometer with measurement channels at 380, 500, 875, and 945 nm and a "peak hold" capability was used as a companion instrument to the PARABOLA. The direct solar beam saturates the PARABOLA detectors for the pixel at that view angle, and therefore a separate measurement of the Sun is required for computations of direct and total irradiant flux. The Sun photometer data were used to compute the atmospheric aerosol optical thickness at PARABOLA wavelengths, which were then used to compute direct beam irradiance. The Sun photometer used in this study was a type referred to as a "Miami" unit (University of Florida; Professor J. Prospero). Spectral peak wavelengths used in this study were at 500 and 875 nm.

B. Measurement and Computation of Direct and Diffuse Irradiance

The direct beam irradiance was computed using values of aerosol optical depth inferred from sunphotometer, total precipitable water from the nearest radiosonde stations on the experiment date and the climatological monthly average value of total ozone. The formulations for rayleigh, water vapor, ozone, and aerosol transmittances given by Bird [9] were used with the previously mentioned inputs. Further detail on this application of direct irradiance computation is given in Deering and Eck [10].

The hemispheric diffuse irradiance was computed from an integration of the sampled directional measurements made by the PARABOLA instrument. Ahmad *et al.* [11] developed an integration technique that involves radiance interpolation in the azimuth and view angle planes from a finite number of directional measurements. Ahmad has shown from simulations that the values of hemispheric diffuse irradiance computed from this technique agree to within 1 to 2% with the true flux obtained from Dave's [12] radiative transfer calculations.

III. STUDY SITE CHARACTERISTICS AND CONDITIONS

The sand shinnery oak (*Quercus havardii*, Rydb.; also referred to as "shin oak"), site (33° 25'N, 102° 50'W) selected for this study was located on the southern high plains region known as the Llano Estacado of West Texas. The shin oak community occurs as a climax vegetation community which

spreads rapidly as the original grassland vegetation disappears with overgrazing. The site selected is a uniform stand of knee high (43.1 cm) woody shrub growing on deep undulating sandy soil. The site was nearly level, with slope ranging from about 0–3%. The plant structure is an open canopy dwarf forest with a substantial underlying "dark" leaf litter layer. A downward viewing camera with a wide angle lens mounted next to the PARABOLA sensor was used to estimate the areal coverage of the vegetation and background. Photos taken on June 6, 1985 were projected onto a dot grid and an estimate of 60.2% vegetation cover was obtained by analyzing the near nadir (0–20° view nadir angle) portion of the photograph.

The sky conditions on September 12, 1984 were mostly cloudless, with an estimated 5–10% cumulus cloud cover on the western horizon at the site, while at the Lubbock, TX regional airport (80 km east of the site) the sunrise to sunset sky cover was given as 10%. The sun was unobscured by cloud throughout the entire field measurement sequence. The resultant wind speed and direction, the vector sum of wind speeds and directions divided by the number of observations, was 6.3 m/s at 180° (southerly) with an average speed of 6.3 m/s as measured at 7.6 m above the ground at Lubbock airport. Air temperature in Lubbock reached a maximum of 33° C and 19° C was the minimum. For the 19 days preceding September 12 there were only 3 days with precipitation, the highest amount being 0.20 cm. This resulted in extremely dry conditions at the site, especially since the sandy soil retains very little moisture.

On the afternoon of June 6, 1985 the estimated sky cover at the site was 5% cumulus and cirrus and the sun remained unobscured by clouds. The wind was much less than on the September measurement date, a resultant speed of 2.1 m/s at 320° (northwesterly) and an average speed of 3.0 m/s as measured at the Lubbock airport. The maximum air temperature was 27° C and the minimum was 14° C. There was a very heavy rainfall on the previous day, June 5, 1985 of 5.60 cm but no precipitation on June 6.

Table I lists the percentages of diffuse irradiance for the range of solar zenith angles when measurements were taken, for the visible and near-infrared wavebands. The percentages of diffuse irradiance was low on both days, with a greater percent diffuse in channel 1 (red waveband), since Rayleigh optical depth increases with decreasing wavelength. On both days, measurements were taken at 62° solar zenith angle and Table I shows that there was a higher percentage diffuse irradiance (ch. 1) on September 12 with 18.9% for this solar angle than on June 6 with 10.5%. This is likely the consequence of a heavy rain on June 5 that resulted in an aerosol washout, thus yielding a lower aerosol optical depth on June 6 than on September 12. These differences in percentage of diffuse irradiance should be insignificant, however, in their effects on measured reflectance since about 75% or greater of the total irradiance is direct beam irradiance for both days. Also, the previously reported effects of changes in irradiance distribution on reflectance [10] occurred when percent diffuse in the visible was at a much higher percentage, about 65% on the hazy day (57° solar zenith angle) versus approximately 25% on the clear day.

TABLE I
PERCENTAGE DIFFUSE SKY FLUX IN SEPTEMBER AND JUNE AS
COMPUTED FROM PARABOLA DIRECTIONAL SKY MEASUREMENTS

Solar Zenith Angle	Channel 1 (Red; %)	Channel 2 (NIR; %)
June 6, 1985		
50.6	9.0	6.8
62.0	10.5	7.4
70.3	13.7	9.7
September 12, 1984		
31.0	12.4	9.4
45.0	14.4	10.7
62.0	18.9	14.1
71.0	24.2	18.3

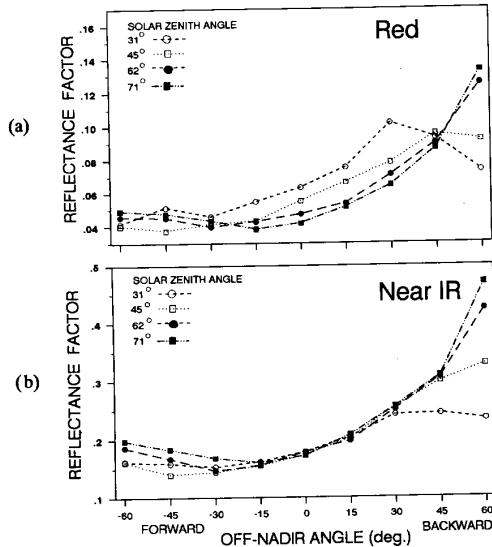


Fig. 1. Solar principal plane bidirectional reflectances in the red (a; 0.662 μm) and near-infrared (b; 0.826 μm) PARABOLA spectral bands for four solar zenith angles.

IV. RESULTS AND DISCUSSION

A. Shin Oak Bidirectional Reflectances — Visible

The solar principal plane bidirectional spectral reflectance of the shin oak community on September 12 at 0.662 μm is shown in Fig. 1(a) for four solar zenith angles ranging from 31° to 71°, and for a view zenith angle range of 0° (nadir) to 60° in both the forwardscatter and backscatter directions. For the view angle range of 15° in the forwardscatter to 30° in the backscatter direction there is a strong trend of decreasing reflectance as solar zenith angle increases.

The trend of decreased reflectance with increase in solar zenith angle can be directly attributable to the increasing amount of shadow that is cast by the vegetation components onto the soil and leaf litter background elements, which have much higher visible reflectances. This shadowing effect on visible bidirectional reflectance has been observed by Deering and Eck [10] in orchardgrass, by Ranson *et al.* [13] in corn, and Pinter *et al.* [6] in wheat canopies. Ranson and Daughtry [14] found that for balsam fir trees arranged on a white background, the red reflectance factor decreased as shadows increased and

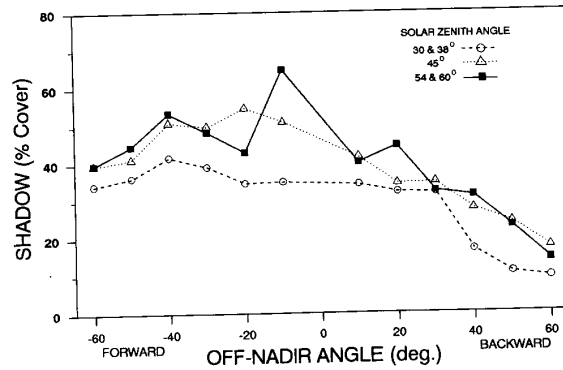


Fig. 2. Photo dot-grid estimates of the percentage of shadow in the sensor view at seven view angles and three solar zenith angles.

that the effect was most pronounced at low percentage cover (sparse) canopies.

The percentage of shadowed scene elements within the shin oak canopy on September 12 was determined by an analyst using projected photograph transparency images on a dot grid matrix. The general trends (Fig. 2) are an increase in percentage shadow as the solar zenith angle increases, for most view angles, and a decrease in percentage shadow from the forwardscatter to the backscatter view directions. This results from the shaded sides of the plants being viewed in the forwardscatter direction.

Otterman's [15] model of a plane with vertical, cylindrical protrusions that are completely absorbing and have negligible cross-sectional area was used to compare the modeled effect of shadowing due to solar zenith angle change to the measured changes in reflectance. The protrusion parameter, s , was inferred from the shin oak reflectance data measured at the 31° solar zenith angle, using the method described by Otterman *et al.* [16] and assuming an isotropic soil background. The inferred value of the shin oak community s -parameter is 0.15 using this method. By comparison, a value of 0.12 was inferred for a sand sage plant community [15], and the assumed typical value of 0.15 used by Musick [17] in his studies of arid rangeland.

Once the protrusion parameter is known, the effect of solar-zenith-angle-induced shading effects can be modeled by

$$r_{\theta 2} = \frac{r_{\theta 1}}{\exp[s(\tan \theta_2 - \tan \theta_1)]} \quad (1)$$

where r = nadir reflectance, θ = solar zenith angle, s = protrusion parameter (Otterman, 1981). Equation (1) was used to predict the values of nadir reflectance at 0.662 μm for various solar zenith angles when given the measured nadir reflectance at one solar zenith angle. These model-predicted nadir reflectances are presented in Table II. In the September data set, the observed nadir reflectance at 45° solar zenith angle was used to predict the nadir reflectance at the other solar zenith angles, and for the June data set the nadir reflectance at 50° solar zenith angle was used to predict values at the other available solar zenith angles. From the table it can be seen that there is excellent agreement between predicted and observed nadir reflectance, with percentage differences of only

TABLE II
ESTIMATED EFFECT OF SHADOWS ON NADIR REFLECTANCE (0.662 μm)

Date	Solar Zenith Angle	Nadir Reflectance		
		Observed (%)	Estimated (%)	Percent Difference
Sept. 12	30.8	6.35	5.86	7.7
	45.0 ¹	5.52	—	—
	62.0	4.73	4.84	-2.3
	71.0	4.18	4.15	0.7
June 6	50.0 ¹	5.82	—	—
	62.0	5.22	5.25	-0.6
	70.0	4.72	4.61	2.3

¹Observed value at 45° and 50° solar angles used to estimate reflectance at other solar zenith angles for September 12 and June 6, respectively.

TABLE III
SOLAR ZENITH Θ_s AND AZIMUTH Ψ_s ANGLES FOR THE THREE DATA SETS COLLECTED FOR SHINNERY OAK ON JUNE 6, 1985, TOGETHER WITH THE TOTAL NUMBER OF CR OBSERVATIONS N_{obs} IN EACH DATA SET AND USED IN THE MODEL ANALYSIS

	Set 1	Set 2	Set 3
Θ_s	50.6	62.0	70.3
Ψ_s	273.2	280.0	284.8
N_{obs} measured	62	62	63
N_{obs} used in model	34	34	34

¹The view zenith angles in these observations ranged from 8°-81°; used in model = 8°-60°.

about 2%, except for the predicted value at 31° solar zenith angle in September, which differs from the observed value by about 8%.

In Fig. 1(a) it is also noted that there is a pronounced "hot-spot" reflectance peak at 30° backscatter view nadir angle at the 31° solar zenith angle, and to a lesser extent a peak at 45° backscatter view angle for a solar zenith angle of 45°. These observations agree with the simulations done by Kimes *et al.* [18] of a sparse forest canopy with clumping of vegetation, which closely describes the shin oak canopy with the only major difference being that the shin oak is shrub-height rather than tree-height. As Kimes *et al.* [18] have described, low-transmitting clumps of vegetation in a sparse canopy will cause increased backscatter and decreased forwardscatter relative to a homogeneous canopy. And with a high probability of gap between vegetation elements in a sparse canopy, a soil/leaf litter background that is highly anisotropic with a higher visible reflectance than the vegetation results in a much higher backscatter reflectance for the aggregate scene. Their simulations found that the dominant effect is that of the increased background reflectance contribution for a sparse canopy with a bright background surface. Thus, in Fig. 1(a) the hot-spot peak at 45° in the backscatter view direction for the 45° solar zenith angle is less pronounced than the 30° solar zenith angle peak at the 30° backscatter view zenith angle since a smaller fraction of the background is viewed at 45° view angle and a larger percentage of the background will be shadowed at the 45° solar zenith angle.

The changes in red reflectance due to seasonal vegetation phenology changes are shown in Figs. 3(a) and (c). The visible reflectance is plotted for measurements made at a 62° solar zenith angle on both September 12, 1984 and

June 6, 1985, hereafter simply referred to as September and June, respectively. The measured leaf area index (LAI) in September was 1.75 while in June it was much lower at 0.70. The visible reflectance is lower in September for all view nadir angles (Fig. 3(a)), which is consistent with the higher LAI, since in the visible spectral region leaf reflectance is much lower than the other canopy and background components (sandy soil, litter, branches). The percentage change between September and June visible reflectance was computed as

$$\frac{R_{\text{June}} - R_{\text{Sept}}}{R_{\text{June}}} \times 100\%, \quad (2)$$

where $R_{(\text{date})}$ is the reflectance for a given time period (Fig. 3(c)). It is seen that for large off-nadir view angles of 60° the reflectance is much greater in June (> 22% change). Since at this view angle only the upper canopy layer is being viewed, this change may be due to a greater number of leaves versus branches being viewed in September and possibly due to changes in leaf angle distribution and/or leaf optical properties.

B. Shin Oak Bidirectional Reflectances — Near-Infrared

Fig. 1(b) shows the near-infrared reflectance at 0.826 μm for the measurements made on September 12 for the solar zenith angles ranging from 31° to 71°. In comparison with the visible wavelengths (Fig. 1(a)) the most significant difference is that for the near-infrared the change in reflectance with change in solar zenith angle for the near-nadir view angles of 15° forward-scatter to 30° backscatter is very small and insignificant, as compared to large changes in the visible reflectance. As was discussed in the previous section, the change in visible reflectance was the result of changes in percentage of background area being shadowed. In the near-infrared, however, since the transmissivity of leaves is very high [19] there is almost none of the shadowing effect which is so dominant in the visible. High leaf reflectance in the near-infrared also contributes to multiple scattering within the canopy which results in reduced shadowing. In addition, there is much less contrast in the near-infrared between bright soil and vegetation than in the visible. Huete [20] measured the nadir reflectance over an incomplete green cotton canopy and found that for canopies with light background soils there was a fairly constant near-infrared canopy reflectance for a large change in solar zenith angle.

Thus it is obvious that the protrusion parameter model of Otterman [15] does not apply in the near-infrared for these canopy types, since the protrusions are mainly leaves which have relatively low absorption in the near-infrared. Fig. 1(b) also shows that the hot spot reflectance peak at 30° backscatter for a solar zenith angle of 31° is greatly diminished in comparison to the hot spot in the visible (Fig. 1(a)). For a sparse canopy with a bright background this reduced peak backscatter reflectance is due to soil and leaf litter having a somewhat lower reflectance than the leaves in the near-infrared. Thus the background does not contribute as strong a backscatter component as in the visible.

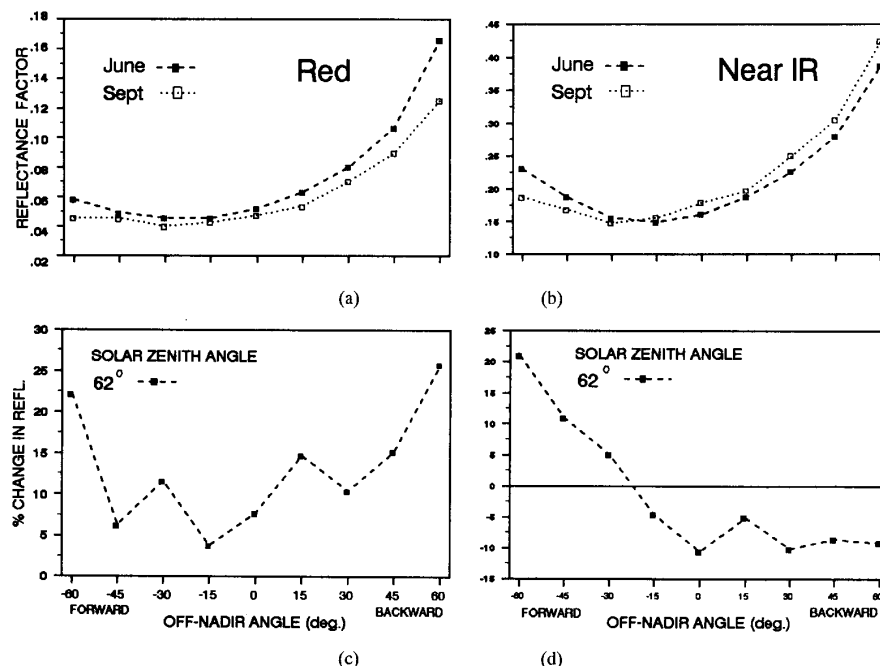


Fig. 3. Solar principal plane red (a) and near-infrared (b) bidirectional reflectances at a 62° solar zenith angle and the corresponding percentage changes in the reflectance factors (c and d) between Fall (1984) and Spring (1985) phenological conditions.

In contrast to the insensitivity of reflectance measurements acquired at near-nadir view angles to variations in solar angle, the near-infrared reflectance at 45° and 60° in the off-nadir backscatter view direction increased substantially as solar zenith angle increased (Fig. 1(b)). This can be attributed to a larger percentage of the irradiance being incident on the top layer of the canopy for large solar zenith angles [21] and only this top canopy layer being viewed at an off-nadir angle of 60°. Also, in comparing the 60° backscatter reflectance magnitude and changes with solar zenith angle to the 60° forwardscatter direction reflectances (Fig. 1(b)) it is apparent that in this canopy there is a very strong preferential scattering in the backscatter direction. For example, at the 71° solar zenith angle the near-infrared reflectance at 60° backscatter view angle is about 47%, which is greater than twice the reflectance measured at 60° in the forwardscatter direction.

Fig. 3(b) is the same as Fig. 3(a) except for the near-infrared rather than the visible wavelength, and it shows the change in reflectance for the shin oak canopy as a function of seasonal phenology changes at a solar zenith angle of 62°. The change in near-infrared reflectance between Sept. and June is consistent with the change in LAI magnitude because a greater LAI in September should result in a higher reflectance, as the leaves are the highest reflectivity scene component in the near-infrared. However, the reverse occurs for the forwardscatter view angles of 30° to 60°, which may be due to increased absorption and, therefore, decreased transmittance when viewing the shaded sides of the leaves. The effect of possible changes in leaf angle distribution (which was not measured) could also be a factor in the observed reflectance changes.

C. Shin Oak Bidirectional Reflectances — NDVI

The Normalized Difference Vegetation Index, or NDVI, was computed using

$$NDVI = \frac{NIR - VIS}{NIR + VIS} \quad (3)$$

where VIS is the visible (red) reflected radiance at 0.662 μm and NIR is the near-infrared reflected radiance at 0.826 μm . The nadir view angle value of the NDVI has been plotted as a function of solar zenith angle for both the September and June measurements in Fig. 4. There is a trend of approximately linearly increasing NDVI with increasing solar zenith angle for both seasons, which can be attributed to the effect of shadowing increasing with solar zenith angle and thus decreasing the visible reflectance, while the near-infrared reflectance remains essentially constant (see Figs. 1(a) and (b)). Therefore, for canopies of this type where the dominant protrusions are green leaves and the background soil has a high visible reflectance, Otterman's [15] model can be used to predict the change in NDVI with change in solar zenith angle. This is done by using the model to calculate the change in visible reflectance due to shading as a result of solar zenith angle changes, and assuming a constant nadir reflectance in the near-infrared as a function of solar zenith angle.

Sellers [22] simulated the effects of solar zenith angle change and leaf-angle distribution change on the NDVI and found that these two factors are predicted to have a large effect at low leaf area indices. For a canopy of LAI = 1 and vertical leaf orientation he computed a nearly linear increase in NDVI with solar zenith angle increase, with a slope that is very similar to the slope of NDVI versus solar zenith angle of the

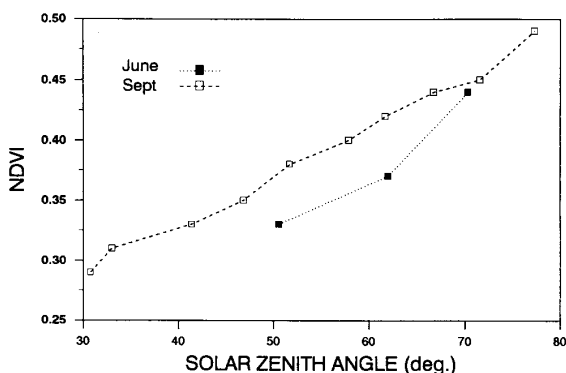


Fig. 4. Nadir-view normalized difference vegetation index (NDVI) changes with solar zenith angle for the two shinny oak sample dates.

September measurements of the shin oak canopy. Although the LAI of the shin oak canopy was 1.75 and the leaves were not all vertically oriented, the canopy is incomplete with a clumped vegetation spatial structure, which presents vertical protrusion elements.

Comparison of the nadir NDVI values for the two seasons (Fig. 4) shows that the NDVI is greater at all solar zenith angles in September, which is expected since the LAI is more than twice as high as in June. It is noted, however, that at 70° solar zenith angle there is only a small difference in the nadir NDVI between the two seasons. This may result from the minimal effect of the soil/litter background at this solar zenith angle, since the background is virtually all in shadow.

The effect of sensor view angle in the solar principal plane on the measurement of the NDVI was also investigated. Figs. 5(a) and (b) shows the NDVI plotted versus view angle from 60° in the forwardscatter direction to 60° in the backscatter direction for a range of solar zenith angles in both seasons. For both dates and all solar zenith angles there is a general trend of NDVI increasing from a minimum in the backscatter view directions to a maximum in the forwardscatter view direction. This is a result of the increasing amount of shadowed area that is viewed in looking toward the forwardscatter direction, which results in a relative decrease in the visible reflectance versus the near-infrared reflectance.

In addition, for both seasons there is a convergence of the NDVI at most solar zenith angles for both the 60° forwardscatter and 60° backscatter directions. These far off-nadir view angles result in very little shadowed background area being viewed at any solar zenith angle and the relative changes in reflectance for both the visible and near-infrared are similar. In Figs. 1(a) and (b) it is seen that there are very large changes in both visible and near-infrared reflectance at the 60° backscatter view angle but that these changes are of relatively similar magnitude in both wavelengths. However, in the near-nadir view angles the visible reflectance changes with solar zenith angle are fairly large, while the near-infrared remain virtually constant, resulting in large changes of NDVI with solar zenith angle. The influence of a hot spot backscattering reflectance maximum in the visible (Fig. 1(a)) in September at the 33° solar zenith angle is seen to correspond to NDVI

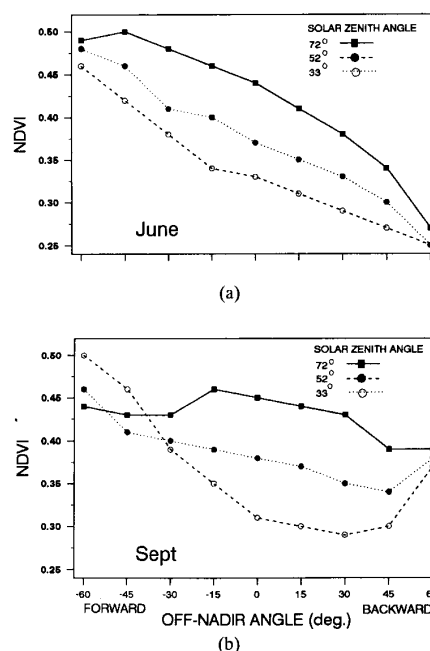


Fig. 5. Shinny oak NDVI computed for the spring (a; 1985) and fall (b; 1984) at three solar zenith angles for off-nadir view angles in the solar principal plane.

minima.

The comparison of the general slopes of NDVI versus view angle between September and June (Figs. 5(a) and (b)) shows that for the solar zenith angle range of 50–72° there is a much steeper slope in June. The largest difference between the NDVI for the two seasons occurs in the backscatter view directions, where at 60° backscatter view direction the NDVI ranges from about 0.37 to 0.39 in September, while in June the NDVI range is approximately 0.25 to 0.27 for this view angle. This extreme change in the far off-nadir backscatter direction NDVI can be attributed to the much higher LAI in September. The higher LAI results in an increased near-infrared reflectance and a substantially decreased visible reflectance, which is pronounced at the far off-nadir view angle, since only the top canopy layer is viewed and the background effects are minimal. This leads to accepting the intuitive conclusion that off-nadir viewing remote sensing is more sensitive to the plant characteristics, which are relatively unadulterated by the background.

D. Model Fit and Inversion for Biophysical Parameters

In the previous works of one of this paper's authors a method was developed for estimating important biophysical variables, such as leaf area index (LAI) and percentage of ground cover (GC) for homogeneous as well as inhomogeneous two- and three-dimensional vegetation canopies. The technique involves the inversion of a canopy reflectance (CR) model using measured bidirectional CR data in the near-infrared region. The model, which is referred to as TRIM, for Three-dimensional Radiation Interaction Model, and its

TABLE IV
VALUES OF THE CANOPY PARAMETERS ESTIMATED THROUGH INVERSION OF THE HOMOGENEOUS MODEL TOGETHER WITH THE AVAILABLE CORRESPONDING MEASURED VALUES. (SKYL WAS KEPT FIXED AT ITS MEASURED VALUE THROUGHOUT. ALSO GIVEN ARE THE MEASURES OF FIT, PRMSE, FOR EACH DATA SET AND THE NUMBER OF OBSERVATIONS N_{obs} USED IN THE INVERSION PROCESS)

Canopy Parameters	Estimated Values			Average \pm Std. Dev.	Measured Values
	Set 1	Set 2	Set 3 ²		
LAI	1.06	1.04	1.05	1.05 ± 0.01	0.70
ρ	0.43	0.40	0.37	0.4 ± 0.03	0.55
τ	0.21	0.25	0.29	0.25 ± 0.04	0.39
ρ_s	0.18	0.17	0.15	0.17 ± 0.01	0.40
μ	0.40	0.70	1.00	0.7 ± 0.3	—
ν	2.60	2.70	2.60	2.6 ± 0.4	—
ALA	77.1°	68.7°	65.8°	$71.4^\circ \pm 5.7$	—
PRMSE	5.7	6.4	6.6	6.2 ± 0.5	—
N_{obs}	34	34	34		
Measured Values of Skylight					
SKYL	0.068	0.074	0.097		

¹Only observations with view zenith angle $\leq 60^\circ$ were used in the inversion process.

²For data set 3 ρ_s was kept fixed at 0.15 during inversion.

application to soybean, corn, black spruce, and orchardgrass canopies are described in a series of papers [23]–[29]. In this analysis, we present the results of the application of this procedure to the shin oak canopy, using the PARABOLA's near-infrared data. The reader is reminded that the field data acquisitions were acquired long before the model development, and therefore measurements of all desired model parameters were not acquired.

Although the model and the inversion technique are fully detailed in the papers mentioned above, for the convenience of the reader we briefly review them here. The model can be used in two ways: first, to model CR of canopies which are assumed to be homogeneous and secondly, to allow for inhomogeneities which may be present in the canopy, such as in row planted vegetation. Our focus in this analysis is on the homogeneous form, since the shinnery oak is a natural, “randomly” distributed vegetation type.

When the canopy is assumed to be homogeneous, the model uses seven parameters: leaf hemispherical reflectance, ρ , and transmittance, τ , LAI, two parameters μ and ν describing the leaf angle distribution which is approximated by a beta distribution [30], soil hemispherical reflectance, ρ_s , and fraction of incident diffused skylight, SKYL. We refer to this form of the model as the “homogeneous model.”

The inversion procedure essentially consisted of carrying out a least squares fit of the model to CR data collected for a sufficient number of solar/view directions (typically 7 to 25). We measure the success of the technique in two ways:

- 1) How well do our estimates of the canopy parameters compare with the corresponding measured values?
- 2) How well do the calculated CR's (using the model with the estimated parameter values) compare with the corresponding measured values? The measure we use here is PRMSE, the percent root mean square error between the measured and calculated CR's defined by

$$\text{PRMSE} = \left[\sum (1 - R_c/R_m)^2 / N_{\text{obs}} \right]^{1/2} \times 100\%. \quad (1)$$

Here R_m is the measured CR for a given solar/view direction, R_c is the corresponding calculated canopy reflectance

(as given by the model), N_{obs} is the number of solar/view directions in a data set and the summation is over all of these directions.

The solar zenith and azimuth angles for the three data sets collected for the shinnery oak canopy are given in Table III. Also given are the total number of observations in each data set. The view zenith angles in these observations range from 8° to 81° . In light of previously experienced deficiencies in the SAIL model (Verhoef [31]; upon which our model is based) for large values of view zenith angle, as a first step in our analysis, we limited the CR data used in the inversion process to observations for which the view zenith angle $\leq 60^\circ$ of which there are 34 in each data set.

With ρ , τ , ρ_s and SKYL fixed at their measured values (see Table IV), we allowed the remaining three homogeneous model parameters LAI, μ and ν to vary freely. In this case, the optimization procedure did not converge (PRMSE $> 100\%$). When we allowed all seven parameters to vary freely, SKYL approached zero. We then fixed SKYL at its measured value and allowed the remaining six parameters to vary. For data sets 1 and 2, the optimization procedure now converged rapidly. For data set 3, however, the value of ρ_s approached zero. We therefore fixed ρ_s at 0.15, a value near the ones estimated for data sets 1 and 2 and repeated the optimization with five parameters free. We then obtained rapid convergence. The results for all three data sets (three solar zenith angles) are given in Table IV. We see that the average estimated value of LAI is 1.05, which is compared with the measured value of 0.70.

It is significant to note that approximately this average value is obtained consistently for each data set thus showing that inversion estimates of LAI were not sensitive to changes in solar zenith angle. (The discrepancy between estimated and measured LAI is discussed below). The average leaf angle (ALA) is 71.4° indicating a highly vertical leaf angle distribution. Unfortunately, we have no available measured value of leaf angle distribution with which to compare these findings. The average estimated values of ρ , τ , ρ_s (0.40, 0.25 and 0.16, respectively) differ significantly from the corresponding measured ones (0.55, 0.39, and 0.40, respectively), and is discussed below.

MEASURED
(Spline
Interpolation)

SHIN OAK — JUNE
CANOPY REFLECTANCE
Sun Zenith = 51°; Sun Azimuth = 273°

MODEL — TRIM
(Homogeneous
Form)

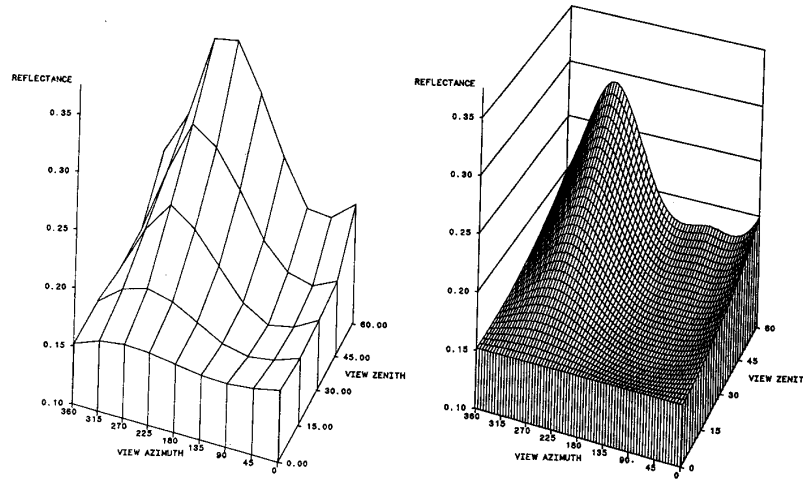


Fig. 6. Measured and modeled bidirectional reflectance surfaces for June 6, 1985 shin oak, $\theta_s = 50.6^\circ$, $\psi_s = 273.2^\circ$: (a) PARABOLA measurements; (b) calculated using the homogeneous model with canopy parameters estimated through inversion with the same model and based on biophysical parameters inferred by the model from the measured CR's.

Although shinnery oak is a naturally growing vegetation, with no apparent row structure, we did investigate the possibility of allowing for inhomogeneities in the canopy by repeating the inversion process, this time, however, using the 3-D row model, which has five additional "canopy geometry" parameters [27], [28]. The average estimated value of LAI was 1.13 and approximately this average value is obtained consistently with all three data sets. In addition, the average PRMSE improved from 6.2% using the homogeneous model to 4.9% when using the row model. The inversion parameter values yielded an estimated value of percentage of ground cover (GC) equal to 64.8%. This is in very good agreement with the value of 60.2% vegetation cover estimated from the analysis of site photographs.

Another measure of the quality of fit is provided in Figs. 6(a) and (b), which are graphs of bidirectional reflectance surfaces for data set 1. In Fig. 6(a), the CR values shown are the measured ones, which have been interpolated for graphing purposes using a bivariate spline. In Fig. 6(b), the CR values shown have been calculated using the homogeneous model with the values of the estimated parameters given in Table IV. As can be seen from this graph, the shape of the calculated bidirectional reflectance surface is very similar to the shape of the measured data surface.

At first glance, it would seem that the average estimated values of ρ and τ (0.40 and 0.25, respectively) are in poor agreement with the measured ones (0.55 and 0.39, respectively). However, the measured values of ρ and τ are for

plant leaves only. We might interpret the average estimated values of ρ and τ to be the values of effective reflectance and transmittance for the entire canopy in the following sense:

$$\rho_e = x\rho_l + (1-x)\rho_b \quad (5)$$

$$\tau_e = x\tau_l + (1-x)\tau_b \quad (6)$$

where ρ_e , ρ_l , ρ_b are effective, leaf, and bark reflectance, respectively (also for transmittance), and x is the fraction of leaves in the canopy and $(1-x)$ is the fraction of bark.

Typical values of ρ_b and τ_b are 0.3 and 0.0, respectively. In carrying out a least square fit of this model to the average estimated values of ρ and τ , we find that the fraction of leaves is 0.61 and the fraction of bark 0.39 (with a PRMSE of 7.4% for this calculation). Thus by interpreting the average estimated values of ρ and τ to be the corresponding ρ_e and τ_e , we obtained reasonable agreement between estimated and measured values of ρ and τ .

Similarly, we may interpret the average estimated value of LAI to be the effective LAI for the entire canopy. Our average estimated value of LAI, 1.05, is higher than the measured value of 0.70, which is for leaves only. This is to be expected, since our estimated value includes a contribution from bark as well. We apply our estimate, computed above, of fraction of leaves as 61% of the total plant material to compute a leaf-only estimate of LAI. The leaf-only LAI estimate is, therefore, the product of the leaf fraction (0.61) multiplied by the estimated LAI (1.05) yielding 0.64 which is very close to the measured LAI.

The average estimated value of ρ_s , 0.16, is significantly different from the measured value of 0.4. This is attributed to the measured value being representative of sand only while the actual ground surface is a mixture of a significant amount of darker leaf litter and the bare sand. Thus it is to be expected that the actual ground surface reflectance would be less than 0.40 since leaf litter reflectance in the near-infrared is relatively low and the litter also shadowed part of the adjacent bare sand area. However, we have no measurements of the combined litter and soil reflectance with which to compare the model-estimated value.

V. SUMMARY AND CONCLUSIONS

Variations in visible and near-infrared reflectance anisotropy due to changes in solar zenith angle and vegetation phenology were observed for a semi-arid shinnery oak plant community. Nadir and near-nadir visible reflectances were found to decrease significantly as solar zenith angle increased due to increased absorption by the canopy and subsequent shadowing of the gap area between plants. A simple model of a plane with absorbing vertical protrusions [15] predicted the visible reflectance change as a function of solar zenith angle. The agreement between predicted and observed visible reflectance was excellent with percentage differences of 8% or less. In the near-infrared waveband, however, the nadir reflectance remained relatively constant as a function of solar zenith angle due to a relative lack of shadowing. This resulted from high leaf transmittance in the near-infrared and multiple scattering due to high leaf reflectance. In response to the solar zenith angle trends of the visible and near-infrared reflectances, the nadir-observed normalized difference vegetation index (NDVI) increased linearly as solar zenith angle increased. The change in NDVI was significant, ranging from 0.29 at 31° solar zenith angle to 0.49 at 77° solar zenith angle, for measurements made in September.

Change in canopy reflectance due to phenology changes were observed from measurements made in June, which is the early-to-middle stage of the growing season, to September, which is near the end of the growing season. The leaf area index was measured to be 0.70 in June and 1.75 in September. Visible reflectance was lower at all view angles in the solar principal plane in September, since leaves are the most highly absorbing component of the canopy. However, in the near-infrared the opposite occurs with higher reflectance in September since leaves are highly reflective relative to other scene elements in this waveband. In the forwardscatter view direction, however, the September near-infrared reflectances were lower than June, possibly due to the reduced transmittance of the leaves at a higher LAI. The nadir NDVI was higher in September when LAI was higher, but at the large solar zenith angle of 70° there was very little difference seasonally since nearly the entire lower canopy and ground surface was shadowed thus reducing the visible waveband contrast between green plant material and background. In both seasons there was a view angle dependence of NDVI from a minimum in the backscatter direction to a maximum in the forwardscatter direction. This was due to the increasing amount of shadowed area viewed in looking off nadir in the forwardscatter direction,

which results in a relative decrease in visible versus near-infrared reflectances.

The measured bidirectional reflectance distribution of near-infrared reflectances were input to a canopy reflectance model which was then inverted to estimate plant canopy biophysical characteristics. The model-estimated value of LAI in June was found to be high (1.05) versus measurements (0.70), but the estimated value was representative of both leaves and stems or branches. When an estimate of the fraction of leaves to fraction of bark-covered branches is made, the adjusted value of estimated leaf-only LAI is 0.64, which is very close to the measured value of 0.70. Even though the shin oak is a naturally growing vegetation community with no discernable row structure, the canopy row model, which allows for inhomogeneities in the canopy, was examined. The inversion result of 65% canopy cover for the shin oak canopy is in very good agreement with the value of 60% vegetation cover estimated from photographic analysis. More comprehensive data sets are needed with additional vegetation types to fully evaluate the utility of these and other plant canopy models.

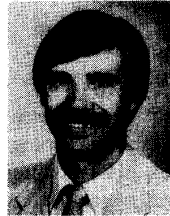
ACKNOWLEDGMENT

Computational work for the model data analysis was carried out on the Watson School's IBM 4381 at SUNY Binghamton during T. Grier's work on the Ph.D. degree, and we greatly appreciate the school's support for this research effort. Special thanks is extended to Dr. Russ Pettit, Texas Tech University, Lubbock, TX for his helpful advice and assistance with the important contacts with the local ranchers and others that enabled us to collect the data in Texas. We also thank Babu Banerjee of ST Systems Corporation for support with computer graphics.

REFERENCES

- [1] D. W. Deering and P. Leone, "Sphere scanning radiometer for rapid directional measurements of sky and ground radiance," *Remote Sensing Environment*, vol. 19, pp. 1-24, 1986.
- [2] C. J. Tucker, C. O. Justice, and S. D. Prince, "Monitoring the grasslands of the Sahel 1984-1985," *Int. J. Remote Sensing*, vol. 7, pp. 1571-1581, 1986.
- [3] J. Otterman and C. J. Tucker, "Satellite measurements of surface albedo and temperature in semi-desert," *J. Climate and Applied Meteorology*, vol. 24, pp. 228-235, 1985.
- [4] E. M. Middleton, "Solar zenith angle effects on vegetation indices and estimates of canopy variables in tall grass prairie," *Remote Sensing Environment*, in press, 1991.
- [5] R. D. Jackson, P. M. Teillet, P. N. Slater, G. Fedosejevs, M. F. Jasinski, J. K. Aase, and M. S. Moran, "Bidirectional measurements of surface reflectance for view angle corrections of oblique imagery," *Remote Sensing Environment*, vol. 32, pp. 189-202, 1990.
- [6] P. J. Pinter, R. D. Jackson, S. B. Idso, and R. J. Reginato, "Diurnal patterns of wheat spectral reflections," *IEEE Trans. Geosci. Remote Sensing*, vol. 21, pp. 156-163, 1983.
- [7] K. J. Ranson and C. S. T. Daughtry, "Scene shadow effects on multispectral response," *IEEE Trans. Geosci. Remote Sensing*, vol. 25, pp. 502-509, 1987.
- [8] A. R. Huete, "Soil and sun angle interactions on partial canopy spectra," *Int. J. Remote Sensing*, vol. 8, pp. 1307-1317, 1987.
- [9] R. E. Bird, "A simple, solar spectral model for direct-normal and diffuse horizontal irradiance," *Sol. Energy*, vol. 32, pp. 461-471, 1984.
- [10] D. W. Deering and T. F. Eck, "Atmospheric optical depth effects on angular anisotropy of plant canopy reflectance," *Int. J. Remote Sensing*, vol. 8, no. 6, pp. 893-916, 1987.

- [11] S. P. Ahmad, E. M. Middleton, and D. W. Deering, "Computation of diffuse sky irradiance from multidirectional radiance measurements," *Remote Sensing Environment*, vol. 21, pp. 185–200, 1987.
- [12] J. V. Dave, "Extensive dataset of the diffuse radiation in realistic atmospheric models with aerosol and common absorbing gases," *Sol. Energy*, vol. 21, pp. 361–369, 1978.
- [13] K. J. Ranson, L. L. Biehl, and M. E. Bauer, "Variation in spectral response of soybeans with respect to illumination, view and canopy geometry," *Int. J. Remote Sensing*, vol. 12, pp. 1827–1842, 1985.
- [14] K. J. Ranson, C. S. T. Daughtry, L. L. Biehl, and M. E. Bauer, "Sun-view angle effect on reflectance factors of corn canopies," *Remote Sensing Environment*, vol. 18, pp. 147–161, 1985.
- [15] J. Otterman, "Plane with protrusions as an atmospheric boundary," *J. Geophys. Res.*, vol. 86, pp. 6627–6630, 1981.
- [16] J. Otterman, D. Deering, T. Eck, and S. Ringrose, "Techniques of ground-truth measurements of desert-scrub-structures," *Advances in Space Research*, vol. 7, no. 11, pp. 153–158, 1987.
- [17] H. B. Musick, "Temporal change of Landsat MSS albedo estimates in arid rangeland," *Remote Sensing Environment*, vol. 20, pp. 107–120, 1986.
- [18] D. S. Kimes, W. W. Newcomb, R. T. Nelson, and J. B. Schutt, "Directional reflectance distributions of a hardwood and pine forest canopy," *IEEE Trans. Geosci. Remote Sensing*, vol. 24, pp. 281–293, 1986.
- [19] H. W. Gausman, R. R. Rodriguez, and A. J. Richardson, "Infinite reflectance of dead compared with live vegetation," *Agron. J.*, vol. 68, pp. 295–296, 1976.
- [20] A. R. Huete, "Soil-dependent spectral response in a developing plant canopy," *Agron. J.*, vol. 79, pp. 61–68, 1987.
- [21] D. S. Kimes, "Dynamics of directional reflectance factor distributions for vegetation canopies," *Appl. Opt.*, vol. 22, pp. 1364–1372, 1983.
- [22] P. J. Sellers, "Canopy reflectance, photosynthesis, and transpiration," *Int. J. Remote Sensing*, vol. 6, pp. 1355–1372, 1985.
- [23] N. S. Goel and R. L. Thompson, "Inversion of vegetation canopy reflectance models for estimating agronomic variables V. Estimation of LAI and average leaf angle using measured canopy reflectance," *Remote Sensing Environment*, vol. 16, pp. 69–85, 1984.
- [24] N. S. Goel and D. W. Deering, "Evaluation of a canopy reflectance model for LAI estimation through its inversion," *Proc. IEEE Trans. Geosci. Remote Sensing*, vol. GE-23, pp. 674–684, 1985.
- [25] N. S. Goel and T. Grier, "Estimation of canopy parameters for inhomogeneous vegetation canopies from reflectance data I. Two-dimensional row canopy," *Int. J. Remote Sensing*, vol. 7, pp. 665–681, 1986.
- [26] N. S. Goel and T. Grier, "Estimation of canopy parameters for homogeneous vegetation canopies from reflectance data II. Estimation of leaf area index and percentage of ground cover for row canopies," *Int. J. Remote Sensing*, vol. 7, pp. 1263–1286, 1986.
- [27] T. Grier, "Estimation of biophysical parameters for inhomogeneous vegetation canopies from reflectance data," doctoral dissertation, State University of New York, Binghamton, NY, 1987.
- [28] N. S. Goel and T. Grier, "Estimation of canopy parameters for inhomogeneous vegetation canopies from reflectance data III. TRIM: A model for radiative transfer in heterogeneous three-dimensional canopies," *Remote Sensing Environment*, vol. 25, pp. 255–293, 1988.
- [29] N. S. Goel and T. Grier, "Estimation of canopy parameters of row planted vegetation canopies using reflectance data for only 4 view directions," *Remote Sensing Environment*, vol. 21, pp. 37–51, 1987.
- [30] N. S. Goel and D. E. Strebel, "Simple beta distribution representation of leaf orientation in vegetation canopies," *Agron. J.*, vol. 76, pp. 800–803, 1984.
- [31] W. Verhoef, "Light scattering by leaf layers with application to canopy reflectance modeling: SAIL model," *Remote Sensing Environment*, vol. 16, pp. 125–141, 1984.



Donald W. Deering received the B.S. and M.S. degrees from Texas Tech University in 1970 and 1972, respectively. He received the Ph.D. degree in range science with an emphasis in remote sensing in 1978 from Texas A&M University.

Since joining NASA's Goddard Space Flight Center in 1978, he has been active in the development of field radiometry instrumentation and techniques and studying the bidirectional reflectance characteristics of land surface covers and their relationships to biophysical and climatic variables. He is currently leading a team of 10 U.S. scientists in an international project in the Soviet Union, where the use of remote sensing for land surface climatology in the steppe vegetation type is being examined.



Thomas F. Eck received the B.S. degree in meteorology from Rutgers University in 1977 and the M.S. degree in meteorology from the University of Maryland in 1982.

From 1979 to 1981 he worked at Vitro Laboratories in the analysis of active solar energy systems and the performance of thermal solar collectors. From 1982 through the present he has been employed as a contractor, currently with Hughes STX, at the Goddard Space Flight Center. His research interests include the bidirectional reflectance characteristics of natural surfaces, remote sensing of atmospheric water vapor, the distribution of atmospheric aerosols, satellite estimation of insolation, and satellite cloud detection algorithms.

Toby Grier received the B.A. and M.A. degrees in mathematics from Barnard College (1967) and Columbia University (1968), respectively. She completed the Ph.D. degree in advanced technology in the Watson School of Engineering at the State University of New York at Binghamton in 1987.

Her research focus has been in the remote sensing of vegetation through modeling.